

Fast outflows that absorb X-ray and UV radiation are common in AGN and are seen in objects spanning a range of $\gtrsim 10^4$ in luminosity. These outflows are a major component of the nuclear environment, and they may carry a significant fraction of the accretion power. In luminous Broad Absorption Line quasars (BALQs) outflows are observed to reach velocities up to a few 10^4 km s $^{-1}$, and they subtend ≈ 10 –30% of the sky as viewed from the central source. In lower-luminosity Seyfert galaxies, outflows are observed $\gtrsim 50\%$ of the time, although they have considerably lower velocities (up to $\approx 10^3$ km s $^{-1}$). The connection between the modest outflows in Seyfert galaxies and the energetic winds in high-luminosity, high-redshift BALQs remains poorly understood (e.g., Laor & Brandt 2002). Are the outflows in these two populations extremes of a continuum or are they qualitatively different?

Grating X-ray spectroscopy of ≈ 20 nearby Seyfert galaxies has led to major advances in understanding their outflows (e.g., see Brandt & Kaspi 2002 for a recent review). More than 140 unique X-ray absorption and emission transitions have been detected and used to constrain outflow dynamics, geometry, and physical conditions. Seyfert galaxy X-ray absorbers are generally observed to be outflowing with velocities comparable to those of their UV absorbers.

Grating X-ray spectroscopy of the more luminous and distant BALQs, however, has not been performed due to photon starvation. This is particularly unfortunate, since BALQ outflows are faster and are probably much more powerful than those in nearby Seyferts. The current X-ray spectra of BALQs, obtained with CCD detectors, show that heavy X-ray absorption is often present (e.g., Gallagher et al. 2002); the X-ray absorption is usually much stronger than that seen from Seyfert outflows. However, the dynamical state of this absorption is generally unknown due to limited spectral resolution; the X-ray absorbing material could be outflowing as part of the wind or relatively stationary at its base (e.g., Murray et al. 1995). This lack of X-ray dynamical information prevents reliable estimation of the wind’s total kinetic luminosity and mass outflow rate; these quantities remain uncertain by a factor of $\gtrsim 100$. Because the column densities of BALQ X-ray absorbers appear to be generally much higher than those of their UV absorbers, the X-ray absorbing material could easily be the dominant contribution to the kinetic luminosity and mass ejection rate if it is indeed outflowing. Furthermore, without dynamical information on the X-ray absorber we cannot investigate relations between the X-ray and UV absorption properly. **Grating X-ray spectroscopy of a luminous AGN outflow, while observationally intensive, can provide a unique, qualitative advance in understanding. It is the logical next step after the Seyfert grating results for a qualitative advance.**

Proposed Observation and Science Goals

We propose an ambitious 350 ks *XMM-Newton* observation of the $z = 0.087$ radio-quiet quasar PG 1351+640 ($M_V = -23.3$ for $H_0 = 70$ km s $^{-1}$ Mpc $^{-1}$); this is a “large program” following §5.9 of the “AO3 Policies and Procedures” document. The main goal of this observation is to obtain a grating-resolution spectrum that will constrain critically important X-ray absorption parameters, and the superb EPIC data will also be intensively utilized to study X-ray spectral features and variability. As described below, we have carefully selected PG 1351+640 as the best target for this long-look *XMM-Newton* observation.

PG 1351+640: *IUE*, *HST*, and *FUSE* studies of PG 1351+640 have revealed strong and complex UV absorption (e.g., Stocke et al. 1994; Zheng et al. 2001; see Fig. 1a). Broad, blueshifted absorption lines are seen from C III, Ly β , O VI, Ly α , N V, Si IV, and C IV. At least five UV absorption components are observed extending to ≈ 3000 km s $^{-1}$. The UV absorption is substantially broader and more blueshifted than is seen in Seyfert galaxies; Stocke et al. (1994) classify PG 1351+640 as a low-redshift BALQ while Zheng et al. (2001) refer to it as a mini-BALQ. It is thus a critical object that can help to bridge the gap (in both UV absorption properties and luminosity) between the modest outflows in Seyfert galaxies and the energetic winds in high-luminosity, high-redshift BALQs.¹

¹The high-redshift BALQs are simply too X-ray faint for effective *XMM-Newton* grating spectroscopy.

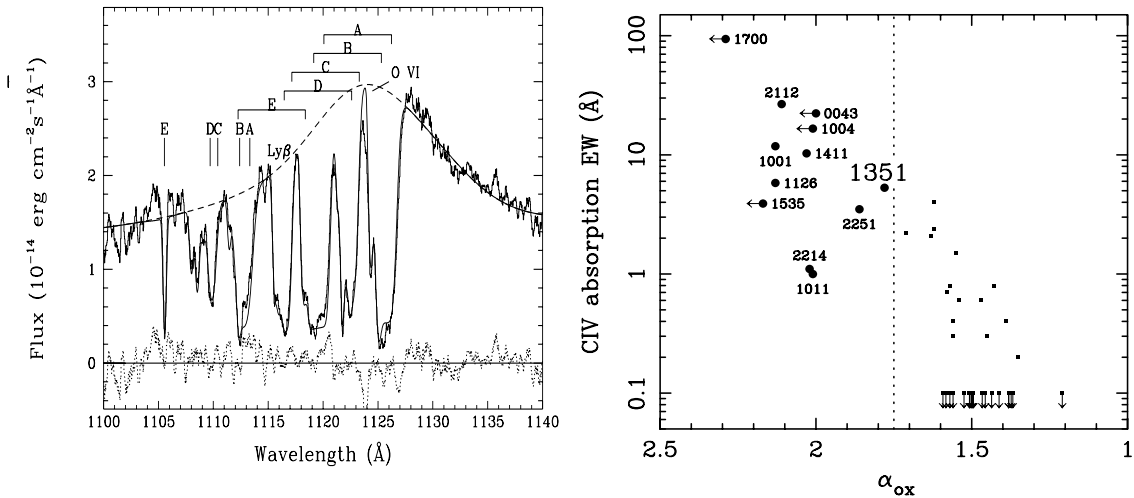


Figure 1: **(a)** O VI absorption in PG 1351+640 as observed by *FUSE* (from Zheng et al. 2001). **(b)** The C IV absorption EW vs. α_{ox} relation for the $z < 0.5$ PG AGN (adapted from Brandt et al. 2000 and Laor & Brandt 2002). The X-ray weak objects with $\alpha_{\text{ox}} > 1.75$ are designated by the right ascension parts of their names; many of these are well-known BALQs or mini-BALQs. Small filled squares are objects with weak or no X-ray and UV absorption. Note the location of PG 1351+640.

The suitability of PG 1351+640 for this project is illustrated in Fig. 1b. In the X-ray band, absorption by outflowing gas often manifests itself by increasing the observed value of α_{ox} , the slope of a nominal power law connecting rest-frame 2500 Å and 2 keV (e.g., Brandt, Laor, & Wills 2000; Gallagher et al. 2001, 2002; Laor & Brandt 2002); AGN with large α_{ox} are weak in the soft X-ray band relative to their optical/UV emission. In a systematic study of the $z < 0.5$ Palomar-Green (PG) AGN, Brandt et al. (2000) discovered a strong correlation between α_{ox} and the EW of blueshifted C IV absorption, supporting the idea that absorption is the primary cause of large α_{ox} (see Fig. 1b). PG AGN with $\alpha_{\text{ox}} > 1.75$ usually show complex X-ray absorption with $N_{\text{H}} \approx 10^{21}\text{--}10^{23} \text{ cm}^{-2}$ when X-ray data with sufficient statistics and spectral resolution are obtained, and there is a one-to-one correspondence between PG AGN that show UV and X-ray absorption. PG 1351+640 has $\alpha_{\text{ox}} = 1.78$ as well as strong UV absorption. It is the **X-ray brightest** PG AGN with $\alpha_{\text{ox}} > 1.75$.

RGS science goals: Directly measuring the dynamics of the X-ray absorbing gas is within reach of the 800–1700 km s⁻¹ resolution of the RGS (see Fig. 2a); the ≈ 15 -fold improvement in resolution from CCD to grating spectra is required to test if the X-ray and UV absorbers share the same dynamics. We expect to detect multiple strong absorption lines from highly ionized N, O, and Ne in the RGS bandpass (e.g., Ly α of H-like and He-like ions); the Doppler shifts of these lines will provide the key dynamical information. For example, strong O VI absorption is seen in the UV (see Fig. 1a), and this ion should create significant X-ray absorption at 21.87 and 22.05 Å. Furthermore, since O VI is not expected to dominate the ionization balance, O VII and O VIII will also likely be seen. As for Seyfert galaxies, the lines observed and their relative strengths will tightly constrain the ionization level of a mini-BALQ X-ray absorber for the first time.

In the widely studied disk-wind model of Murray et al. (1995), the X-ray absorption occurs primarily in stalled, highly ionized “shielding gas” that protects the wind seen in the UV from nuclear EUV and soft X-ray radiation. Without this protective layer, these energetic photons would completely ionize the BAL gas, and the wind seen in the UV could not be driven radiatively. In this model, the X-ray absorber is expected to be highly ionized and should have a much smaller outflow velocity than that of the UV absorber; the outflow’s total kinetic power would correspondingly be much smaller than if the X-ray and UV absorption shared the same dynamics. More recent modeling of this scenario by Proga et al. (2000) suggests that the shielding gas may even be falling toward the black hole which would result in redshifted X-ray absorption lines.

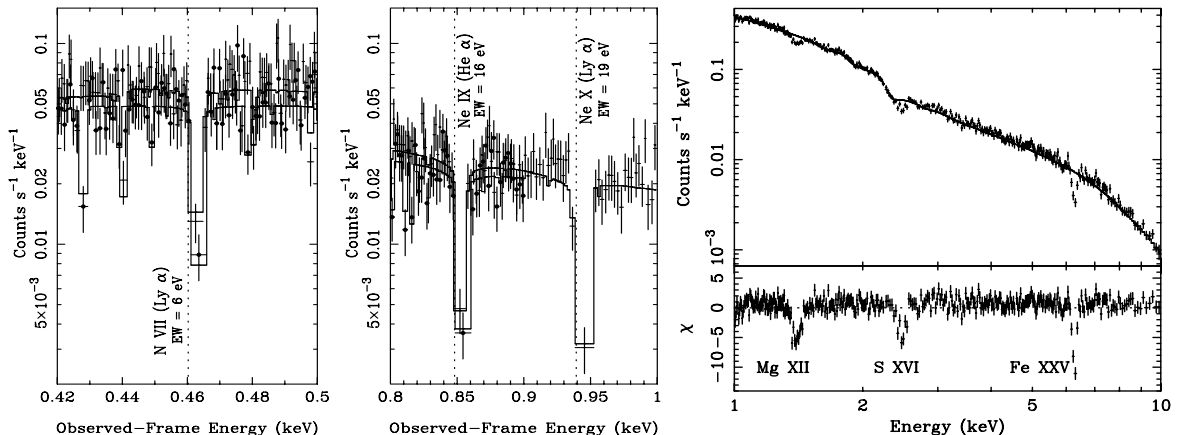


Figure 2: **(a)** The left and middle panels show parts of our simulated RGS1 (filled dots) and RGS2 (plain crosses) spectra along with best-fit models. The labeled dotted lines show expected absorption-line energies in the rest frame of PG 1351+640; note that the blueshift due to outflow (taken to be 1800 km s^{-1} in this simulation) is clearly measurable. The apparent spectral features that are not labeled are due to gaps between the CCDs. **(b)** The right panel shows a simulated EPIC pn spectrum. The model used for the simulation was a $\Gamma = 2$ power law with Mg XII (EW = 15 eV), S XVI (EW = 35 eV), and Fe XXV (EW = 95 eV) absorption lines chosen to have strengths similar to those in Table 1 of Pounds et al. (2003). Note from the residuals that all three lines are clearly detectable.

On the other hand, if the X-ray absorbing gas is part of the outflowing wind (as is the case for Seyfert galaxies), then highly blueshifted X-ray absorption lines should be seen. A high outflow kinetic power would be implied. The bulk velocities and widths measured for these lines should match those seen in the UV ($v_{\text{bulk}} \approx 3000 \text{ km s}^{-1}$ and $\Delta v \approx 2300 \text{ km s}^{-1}$) if there is a tight connection between the X-ray and UV absorbers. Alternatively, the X-ray absorber could represent a more highly ionized gas phase that is outflowing at even higher velocity than the gas seen in the UV. Evidence for such high-velocity X-ray absorbing material with $v_{\text{bulk}} \approx 0.1\text{--}0.4c$ has recently been presented by Chartas et al. (2002) and Pounds et al. (2003). The observed velocity of the X-ray absorber will provide basic information about the radius from which it is launched, and this will be compared with the Broad Line Region and black hole sizes measured for PG 1351+640 by Kaspi et al. (2000). Using both the X-ray and UV data, we will study any connections between the ionization level of the observed gas phases and their dynamics.

EPIC science goals: We expect to gather $\approx 380,000$ counts with the EPIC pn+MOS. These will be the highest quality CCD spectra ever obtained for a mini-BALQ or BALQ, and we will utilize them intensively. For example, we will search for Fe $K\alpha$ and other high-ionization absorption features from the outflow lying at energies above those covered by the RGS (see Fig. 2b). Both Chartas et al. (2002) and Pounds et al. (2003) have recently claimed the detection of strong $> 7 \text{ keV}$ absorption lines from highly ionized iron in quasar outflows; these exciting findings require confirmation and extension to other objects such as PG 1351+640. Pounds et al. (2003) also argue for the detection of blueshifted Mg XII (at 1.49 keV) and S XVI (at 2.69 keV) absorption lines in EPIC spectra of PG 1211+143; these lines should be detectable if present at similar levels in PG 1351+640. Furthermore, we will utilize broad and narrow Fe $K\alpha$ emission lines to constrain the properties of the inner accretion disk and larger scale environment. Finally, any short-timescale flux or spectral variability will constrain nuclear X-ray scattering and the ionization mechanism of the X-ray absorption. PG 1351+640 shows flux and spectral variability on the timescale of $\approx 1 \text{ yr}$ (by $\approx 40\%$; e.g., Rush & Malkan 1996), but rapid variability has not been constrained effectively.

Relevance to other studies: Obtaining the high-quality spectra we propose for PG 1351+640 will enable more sophisticated and physically informed spectral modeling of the ≈ 15 mini-BALQs and BALQs with lower quality X-ray data, advancing this field more generally. Similarly, the 900 ks

Chandra HETGS observation of NGC 3783 (e.g., Kaspi et al. 2002) has served as a touchstone for Seyfert galaxy X-ray studies more generally.

Why XMM-Newton? The large effective area of *XMM-Newton* is required to gather the $\approx 15,000$ – $20,000$ RGS counts needed for an effective X-ray absorption-line study. *Chandra* simply cannot gather the requisite number of counts without a prohibitively long ($\gtrsim 1.5$ Ms) exposure. Furthermore, the simultaneous RGS (0.35–2.0 keV) and EPIC (0.3–10 keV) data that *XMM-Newton* provides will be highly complementary for this project, enabling an effective X-ray absorption study over a broad bandpass. The OM will be used to monitor the UV flux (U, UVW1, UVM2) and to perform low-resolution UV grism spectroscopy.

Supporting data: We will obtain near-simultaneous optical spectroscopy with the 8-m Hobby-Eberly Telescope (30% owned by Penn State). We will also propose for supporting high-resolution UV spectroscopy with *HST* and *FUSE*.

Additional science: This long observation will automatically produce a deep X-ray survey in a low Galactic column density ($N_{\text{H}} = 2.0 \times 10^{20} \text{ cm}^{-2}$) field. We will immediately release the events $> 1.5'$ from PG 1351+640 to X-ray survey researchers, and we will perform follow-up studies.

Technical Feasibility

RGS: We have performed several RGS simulations using SCISIM and XSPEC. The models used in these simulations were based upon the current X-ray data for PG 1351+640 (Rush & Malkan 1996) and similar objects as well as the UV absorption properties of PG 1351+640 (see Fig. 1a). We have adopted an underlying power-law continuum with $\Gamma = 2$ and an unabsorbed 0.1–2.0 keV flux of $1.1 \times 10^{-12} \text{ erg cm}^{-2} \text{ s}^{-1}$. Upon this, we have superposed the expected absorption lines and edges from the ionized outflow. As argued above, for example, we expect strong ($\text{EW} = 5$ – 50 eV) absorption lines from N, O, and Ne in the RGS bandpass. We have set our exposure time so that we will gather 15,000–20,000 source counts from RGS1+RGS2 (the stated range accounts for uncertainties about the ionized absorption). The best photon statistics are obtained over the 0.4–1.3 keV band where we can detect absorption lines with EW down to ≈ 2 – 9 eV . In all of our simulations we find 5–11 absorption lines to be detectable; a few absorption lines from a typical simulation are shown in Fig. 2a. We can measure absorption-line velocities to 300–900 km s^{-1} depending upon line energy and strength; this velocity resolution is clearly sufficient to test if the X-ray and UV absorbers share the same dynamics.

EPIC: Given the model above, we expect count rates of 0.73 ct s^{-1} and 0.36 ct s^{-1} for EPIC pn and MOS1+MOS2, respectively. In total we therefore expect $\approx 380,000$ EPIC counts; these will be the highest quality CCD spectra ever obtained for a mini-BALQ or BALQ. As hoped, our simulations show that we can detect high-energy X-ray absorption lines and other spectral features. In Fig. 2b, for example, we have simulated an EPIC pn spectrum using the continuum model above where we have added three absorption lines similar to those seen from PG 1211+143 by Pounds et al. (2003). All three lines are detected with $> 99\%$ confidence, and we can measure line centroid velocities to within 1900–4100 km s^{-1} . We should be able to detect any strong dependence of line dynamics upon ionization level.

Visibility and other issues: PG 1351+640 is visible for ≈ 88 windows of duration 64–73 ks each during AO3; many of these windows have reasonably low radiation factors. Our observation is therefore within the limits of §5.6 of the “AO3 Policies and Procedures” document. We would prefer that our observation be done over ≈ 6 contiguous windows, but we do not require a formal time constraint. Our OM modes satisfy the brightness and dose constraints.

Brandt W.N., Laor A., Wills B.J., 2000, ApJ, 528, 637 (BLW)
 Brandt W.N., Kaspi S., 2002, in Proc. 16th International Conference on Spectral Line Shapes, 119 (astro-ph/0208248)
 Chartas G., et al., 2002, ApJ, 579, 169
 Gallagher S.C., et al., 2001, ApJ, 546, 795
 Gallagher S.C., et al., 2002, ApJ, 567, 37
 Kaspi S., et al., 2000, ApJ, 533, 631
 Kaspi S., et al., 2002, ApJ, 574, 643

Laor A., Brandt W.N., 2002, ApJ, 569, 641
 Murray N., et al., 1995, ApJ, 451, 498
 Pounds K.A., et al., 2003, MNRAS, in press (astro-ph/0303603)
 Proga D., Stone J., Kallman T.R., 2000, ApJ, 543, 686
 Rush B., Malkan M.A., 1996, ApJ, 456, 466
 Stocke J.T., et al., 1994, AJ, 108, 1178
 Zheng W., et al., 2001, ApJ, 562, 152